Band Gaps in Acoustic Bragg Structures

A. Chiriboga, A. Lindhe-Johan
Department of Physics, Occidental College,
Los Angeles, California 90041
December 5, 2023

Abstract

Acoustic band gaps were observed in a waveguide with four periodic side-loaded stubs using a coherently averaged impulse response. The forbidden transmission bands can be observed by taking the transfer function of a 4000-1000Hz chirp function, a sound pulse that changes frequencies with time. The phase data was then analyzed to determine the acoustic dispersion. These acoustic band gaps agree with theoretical predictions of forbidden frequency intervals and sound wave dispersion.

1. Introduction

Waves define our world, from the smallest particles to the expansion of the cosmos. They describe the most profound phenomena of our universe and the familiar physics of water, springs, and sound. In a pursuit to explain the framework of nature, there has been extensive research in quantum physics related to wave theory. Unfortunately, acoustics has not enjoyed the same level of focus. Yet, as this paper shows, quantum wave theory can often explain the classical physics of acoustics.

Acoustics, the physics of sound, concerns the generation, propagation, and reception of waves in matter. When an acoustic wave propagates in a compressible fluid, molecules are displaced from their equilibrium position, which increases pressure due to compression. This pressure change creates an internal restoring force, like a string's tensile force or a stretched wire's transverse restoring force. These pressure changes propagate through the fluid, enabling the transmission and reception of acoustic waves and creating the phenomenon we know as sound.

Given that all wave mechanics are governed by the same partial differential equation – the wave equation – quantum phenomena often have acoustic analogs.

2. Theory

Acoustic phenomena are often explained using theories pioneered in other fields of physics. These parallels are a result of the universality of wave analysis. This can best be seen in the band gap theory of semiconductors. In semiconductors, two allowed energy bands are separated by a band gap: the valence band (energy level of the valence electrons) and the conduction band, the energy at which the electrons can move freely through the material. The band gap manifests itself as the energy range between the valence and conduction band where no electron states exist. In photonics, "band gaps occur when electron wavefunctions interact with the periodic potential of a crystalline lattice in semiconductors." [1] These band gaps occur when waves in a periodic system interfere and scatter in such a way that there are frequency intervals of forbidden transmission. In acoustics, the same phenomenon of band gaps can be shown by introducing periodic structures to a waveguide. These periodic structures create periodic acoustic impedances. These periodic acoustic impedances cause dispersion of a sound wave in which the speed of a wave depends on the frequency.

Acoustic waves can be described as the propagation of pressure differences within a compressional fluid. In this experiment, we sent an acoustic pulse down an acoustic wave guide filled with air. We can be sure the acoustic wave was a plane wave because in rigid, air-filled, cylindrical waveguides when angular frequencies are below ω_c , often rewritten as frequencies below f_c, only plane waves can propagate. [2]

$$\omega_c = 1.841\frac{c}{a} \tag{1}$$

or

$$f_c = \frac{101}{a} \qquad \text{(for air)} \tag{2}$$

c is defined as the speed of sound (m/s), and a is the radius of the waveguide in meters. This frequency is known as the cutoff frequency, and frequencies above it can create evanescent waves (waves that circulate but do not propagate away). We additionally make the assumption that this experiment is linear and time-invariant. Assuming linearity means that waves can be described using the principle of superposition. Assuming time-

invariance allows for delayed inputs to be expressed as a delayed output. These assumptions can be summed up in 2 equations:

$$ax_1(t) + bx_2(t) \rightarrow ay_1(t) + by_2(t) \tag{3}$$

and

$$x(t - T) \rightarrow y(t - T) \tag{4}$$

where a and b are arbitrary constants, and T represents a delay in time. By making the assumptions of linearity and time independence, we can completely describe the system by its impulse response. A system's impulse response h(t) can describe a system's output $y(t)$ using its input $x(t)$ through a process called convolution (described by $*$).

$$y(t) = x(t) * h(t) \tag{5}$$

The convolution operation can be carried out using the integral below.

$$y(t) = \int_{-\infty}^{\infty} x(\tau)h(t - \tau)d\tau \tag{6}$$

A frequency response $H(f)$ can also completely describe a system's impulse response. $H(f)$ and $h(t)$ are known as Fourier transform pairs where:

$$h(t) = \mathscr{F}(H(f)) = \frac{1}{\sqrt{2\pi}} \int_{-\infty}^{\infty} h(t)e^{itf}df \tag{7}$$

$$H(f) = \mathscr{F}(h(t)) = \frac{1}{\sqrt{2\pi}} \int_{-\infty}^{\infty} H(f)e^{itf}dt \tag{8}$$

with $\mathscr{F}$ representing "the integral operator mapping $h(t) \rightarrow H(f)$." [3] When applying Fourier theory to convolution, we find that the Fourier transform of a convolution is the product of the Fourier transforms.

$$\mathscr{F}(h(t) * H(f)) = \mathscr{F}(h(t))\mathscr{F}(H(f)) \tag{9}$$

This relationship is known as the convolution theorem. [3] Applying this to our impulse and frequency response, we derive that

$$Y(f) = H(f)X(f) \tag{10}$$

and

$$H(f) = \frac{Y(f)}{X(f)}. \tag{11}$$

Moving forward, $H(f)$ will be referred to as the transfer function, with $x(t)$ representing the impulse response of a waveguide system and $y(t)$ representing the impulse response of the periodic impedance system. $X(f)$ and $Y(f)$ are the Fourier transform pairs of $x(t)$ and $y(t)$.

An acoustic impulse response is created by reflections and transmissions inside the waveguide. As an acoustic plane wave travels down a waveguide with side-loaded stubs, it experiences a change in impedance, where some of the wave is transmitted, and some of the wave is reflected. The change of impedance be seen in the presence of evanescent modes in the region of the side-stub. [4] These evanescent modes decay after leaving the vicinity of the side stub. The transmission and reflection of sound in a single side-loaded stub waveguide can be modeled as a pipe that branches into two pipes, each with acoustic impedance Z_1 and Z_2. [5] (See Figure 1) If we set the junction to $x = 0$, the pressures produced at $x = 0$ by the three waves in the pipe are

$$p_i = Ae^{i\omega t} \quad p_r = Be^{i\omega t} \tag{12}$$

and

$$p_1 = Z_1U_1e^{i\omega t} \quad p_2 = Z_2U_2e^{i\omega t} \tag{13}$$

where A and B are the amplitude of the incident and reflected waves in the main pipe, and Z_1, Z_2, and U_1, U_2 are the acoustic impedances and volume velocity complex amplitudes.

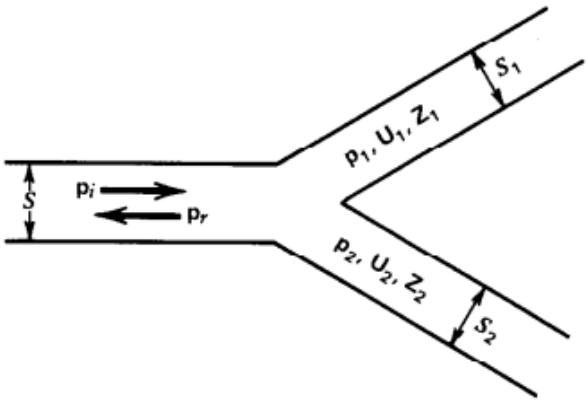

Figure 1: Impedance conditions at a branch. The branches have cross sectional areas $S_1$and S_2 and acoustic impedance's Z_1 and Z_2. [5]

Assuming that the wavelength is long compared to the extent of the complicated flow near the function, we may apply the condition of continuity of pressure to the junction and obtain

$$p_i + p_r = p_1 = p_2. \tag{14}$$

The condition of continuity of volume necessitates that

$$U_i + U_r = U_1 + U_2. \tag{15}$$

Acoustic systems can be thought of in electrical analogs. For example, the pressure difference across an acoustic element can be thought of as the voltage in an electrical circuit. The acoustic analog of current is the *volume velocity of a fluid* U, where the fluid can be thought of as a charge. (U is not a vector, so it can't be a velocity,

but this nonetheless is the convention)[5] Acoustic impedance, **Z**, of a fluid acting on a surface area S is defined as the acoustic pressure divided by the volume velocity at the surface.

$$Z_0 = \frac{p}{U} \tag{16}$$

Dividing Equation 14 by Equation 15 we obtain

$$\frac{U_i + U_r}{p_i + p_r} = \frac{U_1}{p_1} + \frac{U_2}{p_2} \tag{17}$$

which can be rewritten into the form

$$\frac{1}{Z_0} = \frac{1}{Z_1} + \frac{1}{Z_2}. \tag{18}$$

Thus, the combined admittance $1/Z_0$, which describes the flow of acoustic energy, can be expressed as the sum of admittance $1/Z_1$ and $1/Z_2$ of the two side branches.

In the case of a single side-loaded stub connected to a waveguide, the cross sectional area $S_2 = S$. The acoustic impedance of rigid, air-filled, cylindrical waveguide is

$$Z_0 = \frac{\rho c}{S_0} \tag{19}$$

where ρ is the air density, which allows the transmission ratio t and reflection ratio r to be written as

$$t = \frac{p_2}{p_i} = \frac{Z_1}{Z_0 + Z_1} = \frac{Z_1}{\frac{\rho c}{S} + Z_1} \tag{20}$$

and

$$r = \frac{p_r}{p_i} = -\frac{Z_0}{Z_0 + Z_1} = -\frac{\frac{\rho c}{S}}{\frac{\rho c}{S} + Z_1} \tag{21}$$

Using Equations 20 and 21, the acoustic impulse response for a single side-stub waveguide can be calculated. To calculate the impulse response for an N periodic side-loaded stubs, this process must be repeated for every boundary (side-loaded stubs). Using this process, the location of band gaps can be calculated numerically.[6]

The periodicity of N side-loaded stubs creates the necessary conditions for the application of Floquet's Theorem. Floquet's theorem can be applied to two linearly independent systems that are translationally invariant. This can be expressed mathematically:

$$\begin{bmatrix} F(z+h) \\ G(z+h) \end{bmatrix} = \begin{bmatrix} s^{(1)} & 0 \\ 0 & s^{(2)} \end{bmatrix} \begin{bmatrix} F(z) \\ G(z) \end{bmatrix} \tag{22}$$

where $F(z)$ and $G(z)$ represent two linearly independent solutions, h represents the distance between each periodic side-loaded stub, $s^{(1)}$ and $s^{(2)}$ represent eigenvalues, and Equation 22 represents the translation operator operating on the basis composed of $F(z)$ and $G(z)$. Thus the translation relations of $F(z)$ and $G(z)$ are:

$$\begin{aligned} F(z+h) &= s^{(1)} F(z) \\ G(z+h) &= s^{(2)} G(z), \end{aligned} \tag{23}$$

where $s^{(1)} = e^{iqh}$ and $s^{(2)} = e^{-iqh}$, and q is the Bloch wave number or Bloch spatial frequency.[4] This is known as the Bloch wave condition, and the linearly independent wave functions that meet this condition are called Bloch wave functions. Bloch wave functions can be expressed as:

$$\begin{aligned} F(z) &= \Phi_q e^{iNqh} \\ G(z) &= \Phi_{q\_} e^{-iNqh}, \end{aligned} \tag{24}$$

where Φ_q modulates the amplitude of and phase of the spatial frequency q in a periodic manner. Φ_q are generally complex and are referred to as the periodic modulation functions. N refers to the number of periodic side-loaded stubs in the system. By imposing the boundary condition that,

$$\begin{aligned} F(z+Nh) &= F(z) \\ G(z+Nh) &= G(z) \end{aligned} \tag{25}$$

we can use Equation 23 to find that

$$\begin{aligned} e^{iNqh} F(z) &= F(z) \\ e^{-iNqh} G(z) &= G(z) \end{aligned} \tag{26}$$

thus $e^{\pm iNqh} = 1$, or $Nqh = 2\pi n$

$$q = \frac{2\pi n}{Nh}, \qquad (n = 0, \pm 1, \pm 2, ...) \tag{27}$$

The acoustic impedance associated with Bloch waves is called iterative impedance. Because the system is translationally invariant with respect to h, the acoustic impedance must repeat with the periodicity of the structure.[4] The iterative impedance condition is stated mathematically with:

$$Z(z) = Z(z+h). \tag{28}$$

This can be derived by applying the Bloch wave condition to the acoustic pressure and volume velocity of a fluid, such that:

$$\begin{aligned} p(z+h) &= p(z) e^{iqh} \\ U(z+h) &= U(z) e^{iqh} \end{aligned} \tag{29}$$

By applying Equation 16 to the equation above it is clear that the iterative impedance condition is an inherent characteristic of Bloch waves. The dispersion relation can be found by imposing the Bloch boundary conditions on the acoustic field in the periodic media, derived by Bradley as:

$$cos(qh) = cos(kh) - i\frac{Z_0}{2Z_N} sin(kh) \tag{30}$$

where k is the wave number, Z_0 is the impedance in the waveguide, and Z_N is the impedance due to N side-loaded stubs.[4] Plotting this relation gives us the regions of stopbands (disallowed regions) where the dispersion relation does not hold true and passbands (allowed regions) regions where the relation is true. (See Figure 2)

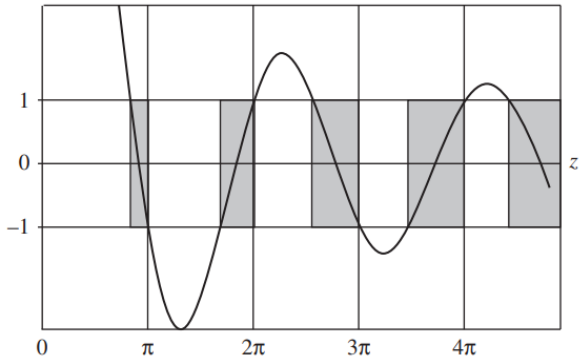

Figure 2: Graph of the dispersion relation for a simplified periodic potential of a crystalline lattice showing passbands (dark regions) separated by stopbands (light regions).[7]

Just as the periodic potential of a crystalline lattice in semiconductors creates band gaps when interacting with electron wavefunctions, so does the periodic acoustic impedance create band gaps when interacting with acoustic wavefunctions.[1] Acoustical band gaps, or stopbands, are "bands of frequencies in which the forward and backward traveling component waves of each cell have equal amplitudes, a longitudinal standing wave condition."[4] This standing wave condition means that at stopband frequencies, the acoustic wave function can be expressed as a "train" of standing waves, where amplitudes vary exponentially with distance. This, along with the dispersion relation, explains the presence of band gaps at certain frequencies, as standing waves do not propagate energy from the source to the destination.

The travelling wave components of a Bloch wave can be described through group velocity and phase velocity. Phase velocity refers to the speed at which a frequency component of a sound wave travels through a medium. Its velocity is dependent on the frequency and can be described as

$$v_p(f) = \frac{c}{n}, \tag{31}$$

where n, the phase refractive index, is a dimensionless factor specific to the frequency that describes how much faster/slower the phase is propagating than the speed of sound. When $n < 1$, the phase propagates faster than the speed of sound, c.[2] On the other hand, group velocity characterizes the speed at which the envelope of a sound wave, representing a collection of frequencies, propagates. In the presence of dispersive media, phase and group velocity will differ. The phase and group velocity relation in Bloch waves is best summarized by Bradley:

"*First, each travelling wave component of a Bloch wave has the same group velocity, and this group velocity is directed in the direction of propagation of the Bloch wave. Second, each travelling wave component of a Bloch wave has a different phase velocity, and this phase velocity can be directed opposite the group velocity!*"[4]

It is important to note that while phase velocities can be greater than c, group velocities will always be less than or equal to c. This is because in linear systems, energy propagates at the same rate as group velocities, and energy is not allowed to be transmitted faster than c.

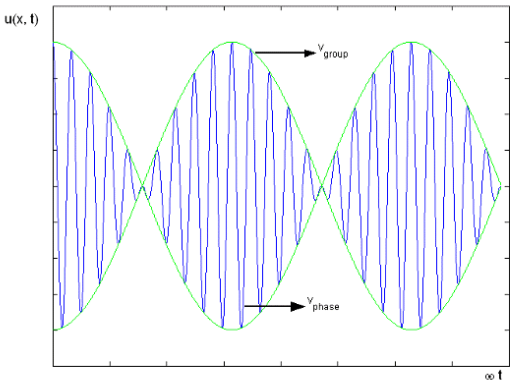

Figure 3: Sample waveform of two sine waves with slightly different frequencies creating beats. This waveform can be characterized by phase (blue) and group (green) velocities.[8]

As seen in Figure 3 above, while the crest of a wave (phase velocity) can move faster than c, the wave packet (group velocity) is bounded by c because information/energy cannot travel faster than c. Using Equation 31, the phase change, $\Delta\phi$, between the frequency responses of a reference and dispersive system of the same length can be modeled by

$$\Delta\phi = (n-1)L\frac{2\pi f}{c} \tag{32}$$

where L is the length of the dispersive system. This equation can then be rearranged to solve for

the phase refractive index, where

$$n = \frac{c\Delta\phi}{2\pi f L} + 1. \tag{33}$$

This equation can be used to calculate the dispersion relation of phase velocity vs frequency. To calculate the group velocity of waves in the waveguide, the definition of velocity was used where D represents the total length of the waveguide and t represents the time from the trigger signal to the first smooth continuous peak above the noise level. To calculate the phase velocity of only the waveguide, the following equation was used

$$v = \frac{L}{\frac{L}{c} + \Delta t} \tag{34}$$

where Δt represents the time difference between the first smooth continuous peak above the noise level of the waveguide and the four periodic side-loaded stubs.

In order to minimize the signal-to-ratio of the experiment, coherent averaging was utilized. Due to the time-invariant nature of the system, each output is identical to the same input signal. By utilizing the fact that noise is not time-invariant, coherent averaging allows for the destructive interference of noise over multiple iterations while constructively preserving the time-invariant waveform.

3. Experimental Method

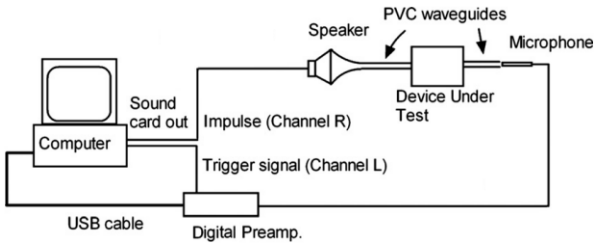

Figure 4: Experimental setup for coherent averaging impulse measurements.[1]

First, we arranged the laptop, speaker, preamp, microphone, and 1/2-inch PVC tubing according to the configuration shown in Figure 4. We then connected the PVC tubes using painter's tape instead of PVC couplers, as the couplers introduce a non-constant cross-sectional area, creating acoustic impedance and dispersion. 3D risers were used to stabilize the PVC waveguide. Making sure that the sound output of the computer was set to Headphone and the sound input was set to Line (Steinberg UR22mlk) we ran one of the provided scripts Matlab[9] by clicking on the Run button. Special care was taken to listen to the pulse coming from the speaker, ensuring that it was repeated ten times. While the script was running, the red peak light on the amplifier was observed to ensure the program ran without triggering the red light, as that indicates data clipping. After the run, we double-checked the plots to ensure there was no clipping.

Next, in MATLAB, we ran the acoustics-script-SINEWAVE.m. The script settings were set to generate an 80ms sine wave snippet with a frequency of 1600 Hz. Other frequencies and wave snippet lengths are possible. Next, we changed the frequency to 800 Hz and repeated the experiment. We then ran acoustics-script-LFMCHIRP.m. This generated a sine wave of decreasing frequency with time. Next, we installed the side-loaded stubs, ensuring that the overall tube remained the same length. We ran acoustics-script-LFMCHIRP.m again, and Fourier analyzed the data to look at phase velocity. We then selected two frequencies within one of the allowed regions, ensuring that there was a significant difference in phase velocities. These two frequencies were then inputted into the acoustics-script-SINEWAVE.m and ran with the four side-loaded stubs.

4. Data

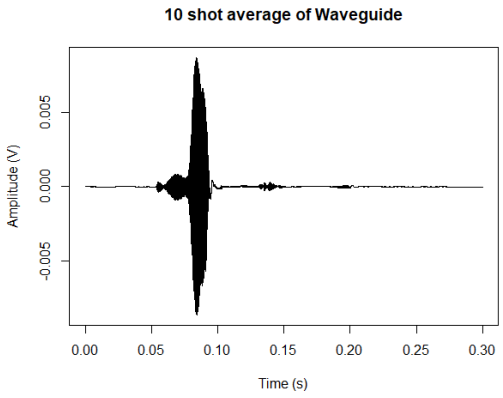

Figure 5: Acoustic impulse response of waveguide from a chirp function coherently averaged 10 times with pulse length 0.08s.

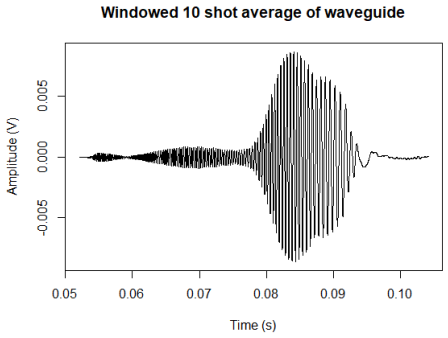

Figure 6: Acoustic impulse response of waveguide from a chirp function windowed to remove reflections coherently averaged 10 times with pulse length 0.08s.

Using a stereo output and impulse signal, the 10-shot average of the waveguide was obtained. The pulse length was set to 0.08s in order to obtain a clean waveform. As can be seen in Figure 5, the main wave packet can be seen from 0.05s to 0.11s, with additional reflections at 0.14s and 0.19s. These reflections and the noise before 0.05s and after 0.11s were windowed out of the Fourier analysis. Figure 6 shows an example of the windowing.

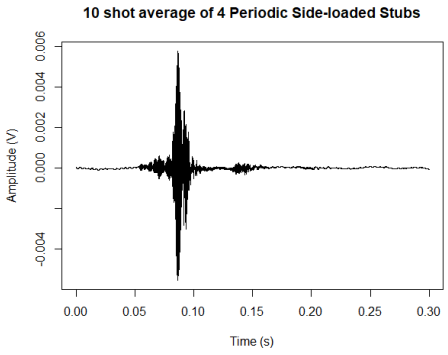

Figure 7: Acoustic impulse response of four periodic side-loaded stubs from a chirp function coherently averaged 10 times with pulse length 0.08s.

The 10-shot average for the four periodic side-loaded stubs was obtained using the same method as above. As can be seen in Figure 7, the main wave packet can be seen from 0.05s to 0.10s, with additional reflections at 0.14s and 0.19s. Note the lack of amplitudes at certain times between Figure 5 and 7. Because the chirp frequencies vary with respect to time, we can see that some ranges are omitted as the chirp frequency sweeps through certain frequencies. These band gaps will be seen more clearly in Fourier analysis. Once again, the reflections and the noise before 0.05s and after 0.10s were windowed out of the Fourier analysis. A windowed and zoomed-in plot of the acoustic impulse of the waveguide can bee seen in Figure 8.

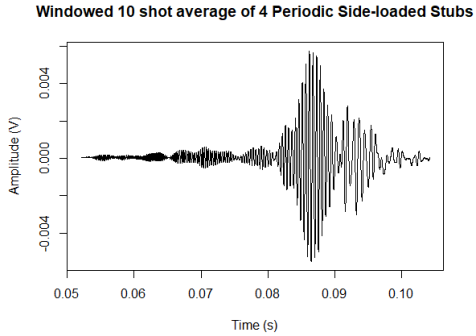

Figure 8: Windowded acoustic impulse response of four periodic side-loaded stubs from a chirp function coherently averaged 10 times with pulse length 0.08s.

Using FFT in RStudio[10], the Fourier transform for the waveguide data, $X(f)$, can be obtained. While there is clearly more prominence in the 1000-2500Hz range, all frequency ranges of the chirp function are displayed.

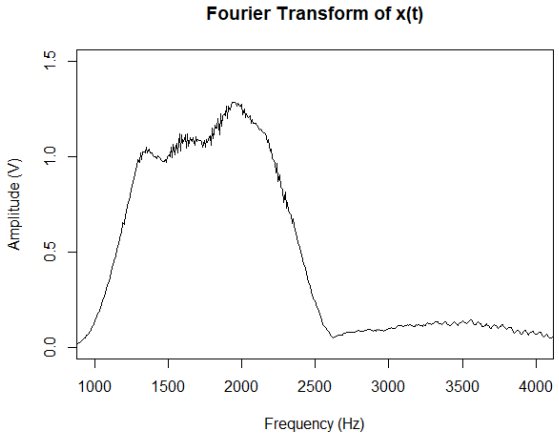

Figure 9: Frequency response of waveguide from a chirp function coherently averaged 10 times with pulse length 0.08s

Looking at the Fourier transform of the four periodic side-loaded stubs, $Y(f)$, it is clear that band gaps are present in the data. These can be clearly seen in ranges of 1500-1700Hz and 2100-2400Hz.

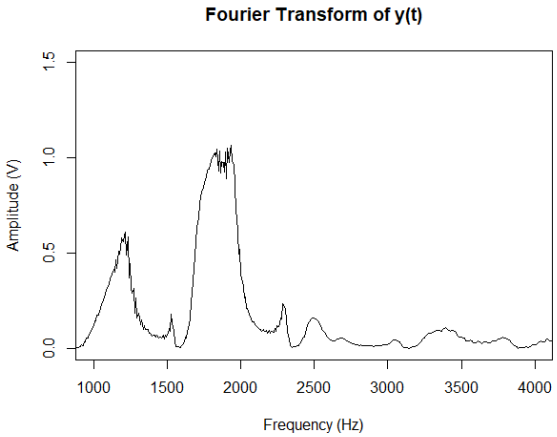

Figure 10: Frequency response of 4 periodic side-loaded stubs from a chirp function coherently averaged 10 times with pulse length 0.08s

The other band gaps can be seen more clearly using Equation 11 to obtain the transfer function. The transfer function is displayed clearly in Figure 11

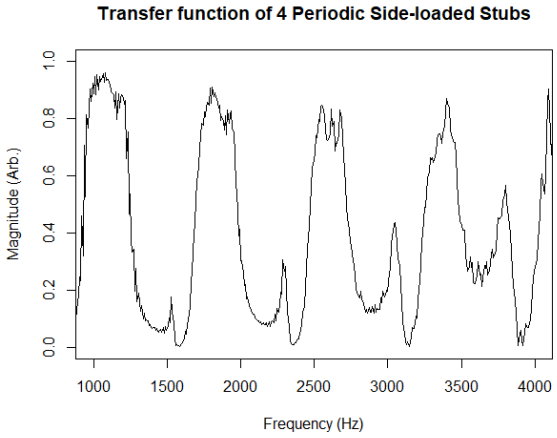

Figure 11: Transfer function that describes the frequency attenuation regions of the four periodic side-loaded stubs.

The raw phase data can be obtained using the angle function in MATLAB on the transfer function and importing it back to RStudio. The angle function in MATLAB is defined as:

$$angle(z) = arctan(Img(z), Re(z)), \qquad (35)$$

where z represents a complex number. The phase data in Figure 12 is noisy in the disallowed regions but smooth and continuous in the allowed regions.

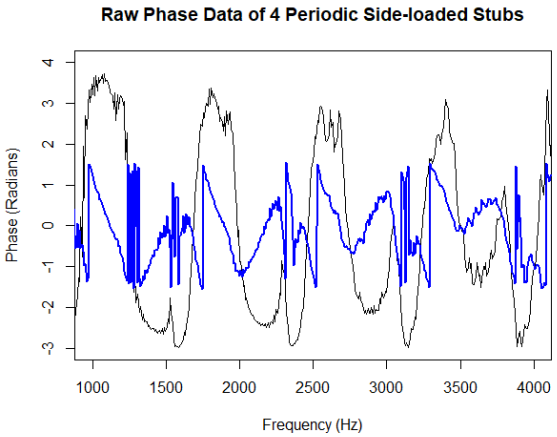

Figure 12: Raw phase data in (blue) derived from the complex transfer function. The magnitude of the transfer function is superposed to show bandgap regions.

Using Equation 31, the phase velocity can be found, which shows a phase velocity below c at the start of allowed regions and a phase velocity above c at the end of allowed regions.

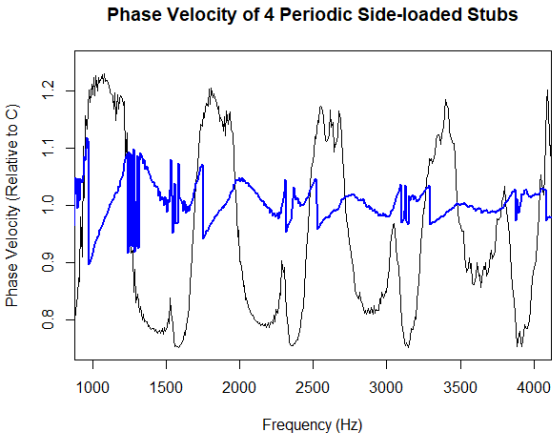

Figure 13: Phase velocity in (blue) derived from Equation 33. The magnitude of the transfer function is superposed to show bandgap regions.

5. Analysis

Table 1: Theoretical vs Experimental Results

Frequency (Hz)	Theoretical (m/s)	Experimental (m/s)
800	343	342.8 ± 0.4
1600	343	342.6 ± 0.4
1025	308	311 ± 9
1200	360	360 ± 10

Analyzing the speed of sound in the waveguide using Equation 34 and measurement.r we found that c was 342.8 ± 0.4m/s at 800hz and 342.6 ± 0.4m/s at 1600Hz. This is within the accepted value of $c = 343$m/s in air at room temperature. To confirm the phase velocity found in Figure 13, a sine wave at 1025Hz and 1200Hz was sent down the waveguide with side-loaded stubs. These frequencies were chosen due to their significant difference in phase velocities. Our model predicted that 1025Hz should be around $0.9c = 308$m/s and $1.05c = 360$m/s at 1200Hz. By taking the first smooth and continuous peak above the noise, we found that the phase velocity at 1025Hz was 311 ± 9m/s and 360 ± 10m/s at 1200Hz. While the uncertainty in time was calculated using an uncertainty of half the sampling time, it is possible that there is a systematic error present in the calculation of the phase velocity. Nonetheless, it is clear the phase velocities tend towards the theoretical phase velocities despite possible systemic error. (Graphs of sine waves for 800Hz, 1025Hz, 1200Hz, and 1600Hz can be seen in the appendix)

6. Discussion

One aspect to consider in the experiment was the appearance of narrow transmission bands in disallowed regions. This is most likely due to the presence of nonperiodic defects in our side-loaded stubs.[11] Measuring the side-loaded stubs, we found that one of our side-loaded stubs was $0.6cm$ off our periodic distance $h = 23.5 \pm 0.1cm$. Additionally, we noticed a sharp fall in amplitude at frequencies above 2500Hz (See Figure 9 and 10). It is possible that this fall-off is caused by a cutoff frequency of the cone that couples the speaker or the waveguide.[2] We last noticed an inconsistency in the system around 800Hz. When the chip function swept over 800Hz, we observed a substantial dip in amplitude on our Fourier graphs. When a sine wave was sent down the pipe at the originally recommended pulse length of 18ms, we were unable to receive an impulse response that resembled a sine wave. We found that increasing the pulse length helped produce a waveform that more closely resembled the 800Hz sine wave sent out by the speaker. Future iterations of this experiment should focus on better insulating the speaker and microphone.

7. Conclusion

Throughout this experiment, analogs from quantum physics were able to help explain the acoustical physics of band gaps and dispersion. Using theory from optics, the experiments were able to show frequency-dependent phase velocity. By imposing Bloch wave conditions, band gaps could be explained. The universality of wave mechanics can not be understated as it underpins the foundations of classical physics to quantum mechanics.

References

[1] W. M. Robertson and J. M. Parker. Acoustic impulse response method as a source of undergraduate research projects and advanced laboratory experiments. *The Journal of the Acoustical Society of America*, 131(3):2488–2494, 2012.

[2] Allan D. Pierce. *Acoustics: An introduction to its physical principles and applications*. Springer, 3 edition, 2019.

[3] Alec J. Schramm. *Mathematical methods and physical insights: An integrated approach*. Cambridge University Press, 2022.

[4] Charles E. Bradley. *Acoustic bloch wave propagation in a periodic waveguide*, 1991.

[5] Lawrence E. Kinsler. *Fundamentals of Acoustics*. Wiley, 4 edition, 2000.

[6] M. S. Kushwaha, A. Akjouj, L. Dobrzynski, B. Djafari-Rouhani, and J. O. Vasseur. Acoustic spectral gaps and discrete transmission in slender tubes. *The Journal of the Acoustical Society of America*, 104:1745–1745, 1998.

[7] David J. Griffiths and Darrell F. Schroeter. *Introduction to quantum mechanics*. Cambridge University Press, Cambridge ; New York, NY, third edition edition, 2018.

[8] Maria Dworzecka. Phase and group velocities. *Phase and group velocity*.

[9] The MathWorks Inc. Matlab version: 9.13.0 (r2022b), 2023.

[10] RStudio Team. *RStudio: Integrated Development Environment for R*. RStudio, PBC., Boston, MA, 2020.

[11] J. N. Munday, C. Brad Bennett, and W. M. Robertson. Band gaps and defect modes in periodically structured waveguides. *The Journal of the Acoustical Society of America*, 112(4):1353–1358, 2002.

A. Sine Wave Impulse Graphs

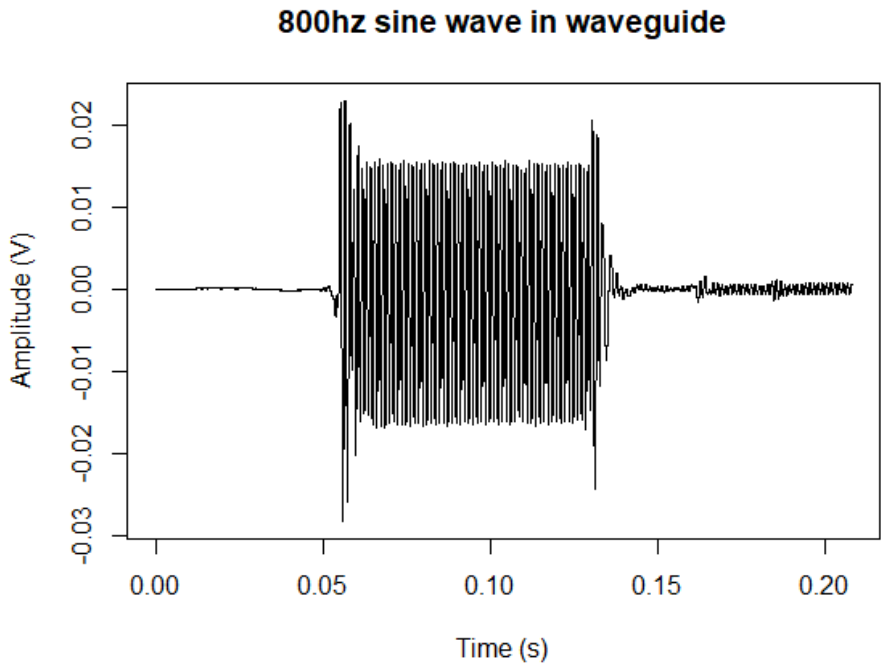

Figure 14: Acoustic impulse response of 800hz sine wave in waveguide

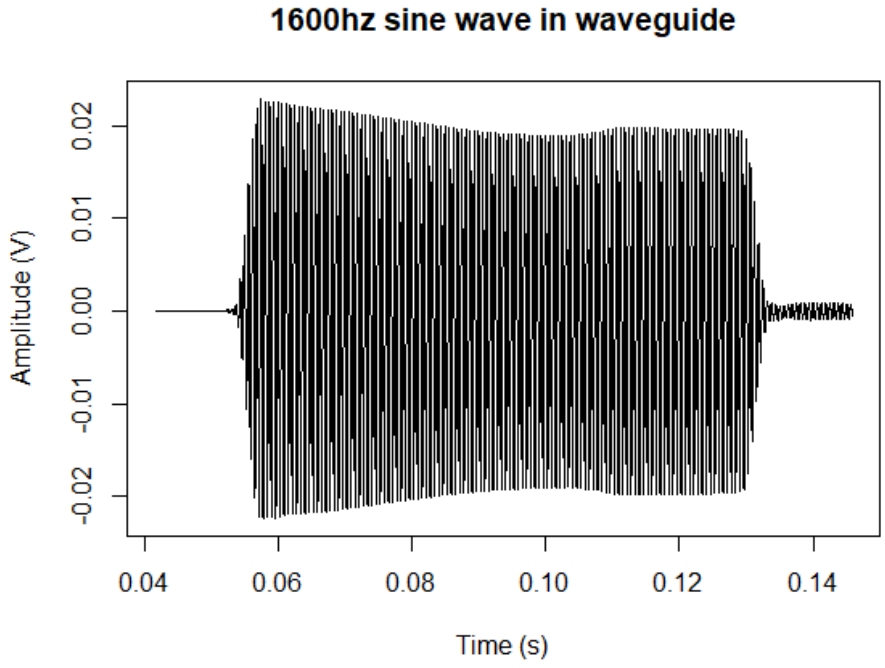

Figure 15: Acoustic impulse response of 1600hz sine wave in waveguide

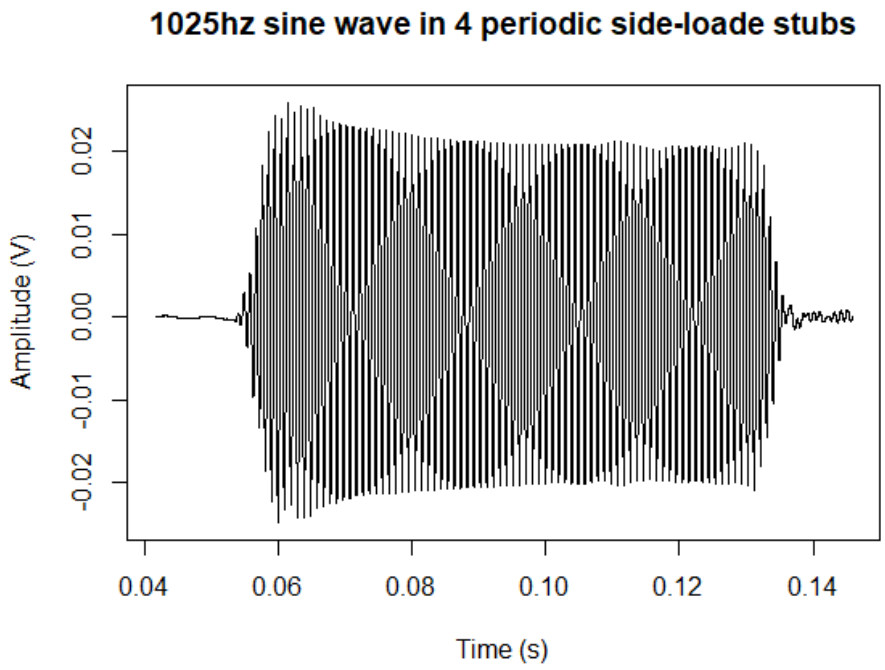

Figure 16: Acoustic impulse response of 1025hz sine wave in four periodic side-loaded stubs

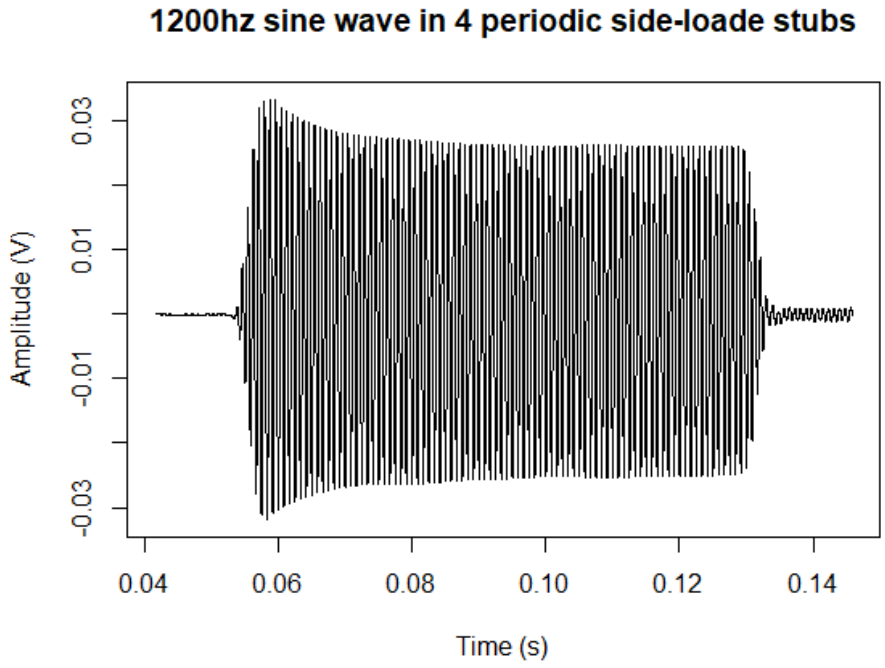

Figure 17: Acoustic impulse response of 1200hz sine wave in in four periodic side-loaded stubs